Journal of Biomechanics 128 (2021) 110700

Contents lists available at ScienceDirect

Journal of Biomechanics

journal homepage: www.elsevier.com/locate/jbiomech

Associations of thrombus perviousness derived from entire thrombus segmentation with functional outcome in patients with acute ischemic stroke

Emilie M.M. Santos [a,b,c,d], Nerea Arrarte Terreros [a,b], Manon Kappelhof [a], Jordi Borst [a], Anna M. M. Boers [a,e], Hester F. Lingsma [f], Olvert A. Berkhemer [a,c,g], Diederik W.J. Dippel [g], Charles B. Majoie [a], Henk A. Marquering [a,b,*], Wiro J. Niessen [c,d,h], on behalf of the MR CLEAN investigators[1]

[a] Department of Radiology and Nuclear Medicine, Amsterdam UMC, Amsterdam, the Netherlands
[b] Department of Biomedical Engineering and Physics, Amsterdam UMC, Amsterdam, the Netherlands
[c] Department of Radiology and Nuclear Medicine, Erasmus Universtiy Medical Center, Rotterdam, the Netherlands
[d] Department of Medical Informatics, Erasmus University Medical Center, Rotterdam, the Netherlands
[e] Institute of Technical Medicine, University of Twente, Enschede, the Netherlands
[f] Department of Public Health, Erasmus University Medical Center, Rotterdam, the Netherlands
[g] Department of Neurology, Erasmus Universtiy Medical Center, Rotterdam, the Netherlands
[h] Faculty of Applied Sciences, Delft University of Technology, Delft, the Netherlands

A B S T R A C T

Thrombus perviousness is strongly associated with functional outcome and intravenous alteplase treatment success in patients with acute ischemic stroke. Accuracy of thrombus attenuation increase (TAI) assessment may be compromised by a heterogeneous thrombus composition and interobserver variations of currently used manual measurements. We hypothesized that TAI is more strongly associated with clinical outcomes when evaluated on the entire thrombus.

In 195 patients, five TAI measures were performed: one manual by placing three regions of interest (TAI_{manual}) and four automated ones assessing densities from the entire thrombus. The automated TAI measures were calculated by comparing quartiles; Q1, Q2, and Q3 of the non-contrast and contrast enhanced thrombus density distribution and using the lag of the maximum of the cross correlations (MCC). Associations with functional outcome (mRS at 90 days) were assessed with univariate and multivariable analyses.

All entire TAI measures were significantly associated with functional outcome with odd ratios (OR) of 1.63(95 %CI:1.19–2.25, p = 0.003) for Q1, 1.56(95 % CI:1.16–2.10, p = 0.003) for Q2, 1.24(95 %CI:1.00–1.54, p = 0.045) for Q3, and 1.70(95 %CI:1.24–2.34, p = 0.001) for MCC per 10 HU increase in univariate models. TAI_{manual} was not significantly associated with functional outcome (p = 0.055). In the multivariable logistic regression models including age, NIHSS, and recanalization, only TAI measures derived from the entire thrombus were independently associated with favorable outcome; OR of 1.64(95 %CI:1.01–2.66, p = 0.048) for Q2 and 1.82(1.13–2.95, p = 0.014) for MCC per 10 HU increase of thrombus attenuation.

The novel perviousness measures of the entire thrombus are more strongly associated with functional outcome than the traditional manual perviousness assessments.

1. Introduction

Thrombus perviousness derived from admission imaging is strongly associated with outcome of acute ischemic stroke treatment (Ahn et al., 2015; Borst et al., 2017; Dutra et al., 2019; Frölich et al., 2012; Kappelhof et al., 2018; Santos et al., 2016b, 2016a). The thrombus perviousness is a qualitative description related to thrombus permeability which is a physical property of thrombi describing the extent of residual flow that can go through the interconnected fibrin filaments, trapped red blood cells, platelets, and other blood constituents (Arrarte Terreros et al., 2020; Bembenek et al., 2017). Thrombus perviousness is determined by the estimation of the level of contrast penetration in a

* Corresponding author at: Department of Biomedical Engineering and Physics, Amsterdam UMC, location AMC, Meibergdreef 9, 1100 AA Amsterdam, the Netherlands.
E-mail address: h.a.marquering@amsterdamumc.nl (H.A. Marquering).
[1] The complete membership of the author group can be found in the Acknowledgments.

https://doi.org/10.1016/j.jbiomech.2021.110700
Accepted 12 August 2021
Available online 28 August 2021

thrombus on radiological imaging (Ahn et al., 2015; Dutra et al., 2019; Kappelhof et al., 2018; Labiche et al., 2003; Santos et al., 2016b, 2016a). In a number of studies, the association of manually determined thrombus attenuation increase (TAI), as assessed on Computer Tomography Angiography (CTA) and non-contrast Computer Tomography (NCCT), with functional outcome and recanalization success has been shown (Menon et al., 2018; Dutra et al., 2019; Kappelhof et al., 2018; Santos et al., 2016b, 2016a; Santos et al., 2018).

The mechanical behavior of thrombi determines the interaction of the thrombectomy device with the thrombus, and therefore, affects endovascular treatment success (Gunning et al., 2018; Mokin et al., 2020). Thrombus perviousness is a measure of a physical property of the thrombus (permeability) and therefore, is related to the biomechanical properties of the thrombus. Previous research has shown that thrombus perviousness is related to thrombus histology (Benson et al., 2020; Berndt et al., 2018; Patel et al., 2021), and that histology is related to the mechanical behavior of thrombi such as fracture, stiffness, or contraction (Fereidoonnezhad et al., 2020; Gunning et al., 2018; Johnson et al., 2020, 2017; Tutwiler et al., 2017). Some studies have shown that higher perviousness is associated with lower RBC content and higher fibrin density (Berndt et al., 2018; Patel et al., 2021); whereas other studies have found the opposite relation: higher perviousness is related to higher RBC content and lower fibrin density (Benson et al., 2020). Higher fibrin content has been associated to fracture toughness (Fereidoonnezhad et al., 2020), stiffness (Johnson et al., 2020) and higher friction coefficient (Gunning et al., 2018; Johnson et al., 2017). Platelet content has previously been related to clot contraction (Johnson et al., 2020; Tutwiler et al., 2017). However, to our knowledge, no study directly relates thrombus perviousness to mechanical behavior of thrombi.

Thrombus perviousness, together with additional thrombus characteristics, was found to be associated with stroke etiology in three recent studies (Boodt et al., 2020; Kufner et al., 2020; Zhang et al., 2020). One study observed higher perviousness values in cardioembolic stroke (Kufner et al., 2020), whereas another reported more 4D-CTA-assessed antegrade flow in large artery atherosclerosis-caused strokes (Zhang et al., 2020).

The combination of the heterogeneous composition of thrombi and the manual techniques used to assess thrombus attenuation may have compromised the accuracy of thrombus perviousness assessment (Santos et al., 2016c). In this study, we employ an automated method to segment the entire thrombus and retrieve the attenuation of all voxels from CTA and NCCT images, which may overcome these problems (Santos et al., 2014, 2016d). We hypothesized that by using this novel approach, TAI can be assessed more accurately on entire thrombus segmentations and therefore may be stronger associated with favorable functional outcome, recanalization, and final infarct volume.

2. Methods & materials

2.1. Patient selection

We retrospectively collected patients from the Multicenter Randomized Clinical trial of Endovascular treatment of acute ischemic stroke in the Netherlands (MR CLEAN) database in which patients were randomly assigned to either best medical treatment alone, including intravenous alteplase if eligible (Control group), or additional intra-arterial treatment (IAT group) (Berkhemer et al., 2015). For inclusion of the patients an occlusion of the anterior large vessel had to be proven on computed tomography (CT_ angiography (CTA), magnetic resonance angiography, or digital-subtraction angiography. The imaging protocols were left to the judgement of the treating teams. Only patients with a proximal intracranial occlusion for whom good quality thin-slice ($\leq$2.5 mm) baseline NCCT and CTA on the same scanner available were included (n = 227). Exclusion criteria for this study were: excessive noise (n = 8), presence of motion artefacts (n = 21), and incomplete region of interest (n = 3), such that 195 patients were included in this study. The MR CLEAN study protocol was approved by the Medical and Ethical Review Committee (Medisch Ethische Toetsings Commissie of the Erasmus MC, Rotterdam, The Netherlands) and the research boards of all participating centers. All patient records and images were anonymized prior to analysis. All patients or legal representatives signed informed consent.

2.2. Thrombus attenuation increase assessments

As thrombus perviousness is a qualitative measure, rather than a physically defined characteristic (WikipediA, 2021). The thrombus perviousness can be considered a derivative of the thrombus permeability. Thrombus perviousness describes to what extent the contrast material, which is administered during CTA acquisition, penetrates the thrombus. Because for the estimation of thrombus permeability a pressure drop along a thrombus is required, this cannot be determined using straightforward radiological imaging (Arrarte Terreros et al., 2020). In this study we assess the thrombus perviousness with measurement of the thrombus attenuation increase (TAI), which is difference in average thrombus attenuation as measured on CTA and measured on NCCT.

CTA and the NCCT were spatially co-registered with Elastix (Klein et al., 2010), using a rigid transformation. If the automated registration was suboptimal, a correction was performed manually (by ES) using Mevislab (Heckel et al., n.d.). Using the co-registered images, TAI measurements were performed with manual and automated assessments. The manual measurement method was performed using 3 regions of interest, whereas the automated method included attenuation values from the entire thrombus (Santos et al., 2016c).

2.3. Manual thrombus attenuation measurement

The manual measurements were performed on NCCT and co-registered CTA by a trained observer (MdB, with 1 year of experience) as previously described (Dutra et al., 2019; Kappelhof et al., 2018; Santos et al., 2016b, 2016a). Using an in-home developed Mevislab (Heckel et al., n.d.) interface in which NCCT and the arterial phase CTA were displayed simultaneously, 3 spherical regions of interests (ROI) with a 1 mm radius were positioned in the proximal, middle and distal part, but away from the boundaries of the thrombus. The ROIs were automatically projected on the other CT images. The mean thrombus attenuation on CTA and NCCT were calculated by averaging the HU of the three ROIs. The observer only had access to baseline NCCT and CTA images and was blinded from measured density and all clinical information.

2.4. Automated entire thrombus attenuation measurement

The entire thrombus was segmented using an adapted semi-automated method (Santos et al., 2014, 2016c). First, the radius along the contralateral vessel was estimated in the co-registered CTA images using an automated vessel segmentation technique with a combination of minimum cost path and graph-cuts. Second, a manual centerline was obtained by interpolating a polynomial curve through manually placed control points in the thrombus using an in home developed Mevislab interface (JB, with four years of experience). Third, a tubular mask was generated around the centerline of the thrombus with the radius of the contralateral arterial segment. Thereafter, within this tube an automatically tuned intensity-based region growing was performed. Subsequently, the resulting thrombus segmentation was smoothed using the mathematical morphological opening operation. Because the images were co-registered, the CTA-based thrombus mask was automatically projected on NCCT. An example patient with both manual annotations and automated segmentation is presented in Fig. 1.

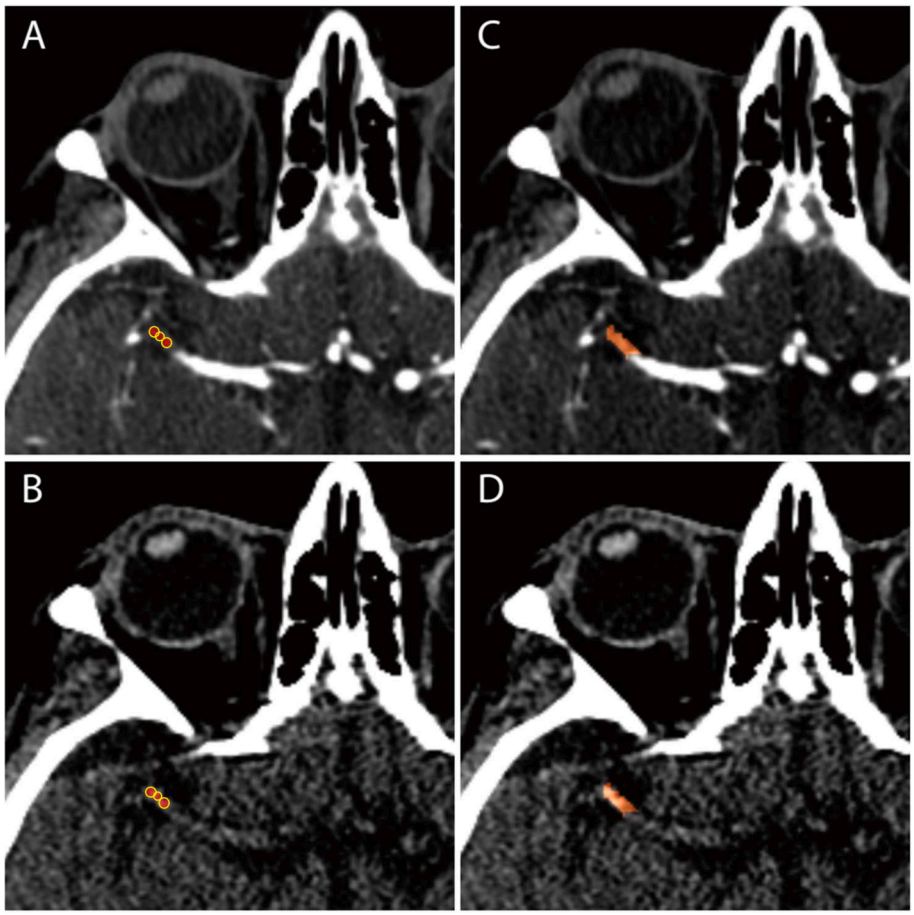

Fig. 1. Example of a co-registered CTA (panel A and C) and NCCT (panel B and D) images of a patient suffering from a right middle cerebral artery occlusion. The red overlay (panel A and B) represents the manually measured density using the three spherical regions of interest. The orange overlay (panel C and D) represents the result of the automated thrombus segmentation on CTA.

2.5. Thrombus attenuation increase measures

Five TAI measures were derived from the manual measurement and automated segmentation: TAI_{Manual}, TAI_{Q1}, TAI_{Q2}, TAI_{Q3} and TAI_{MCC} (Fig. 2). TAI_{Manual} was obtained by subtracting the mean of the three manual ROIs thrombus attenuation measures on NCCT from the mean attenuation from the three ROIs on the CTA. The attenuation distributions of the entire thrombus on NCCT and CTA were represented with quartiles (Fig. 2). TAI_{Q1}, TAI_{Q2} and TAI_{Q3} were obtained by subtracting the first, second, and third quartile of the entire thrombus attenuation distribution on NCCT from the value for CTA. The lag (in HU) of the maximum of the cross-correlation (MCC) between attenuation distributions was calculated using Matlab (Fig. 2). TAI_{MCC} was obtained from the shift between the CTA and NCCT attenuation distribution.

2.6. Outcome measures

The primary outcome, favorable functional outcome, was defined as a score of 2 or less on the modified Rankin Scale (mRS) at 90 days. The mRS is a scale to describe the degree of disability or dependence in a patient's daily activities. It ranges from 0 (no symptoms) to 6 (dead). The score of 2 or less is commonly used to describe functional independence and is commonly name "favorable functional outcome". Secondary outcomes were recanalization, or reopening of the occluded intracranial artery, as expressed with the modified arterial occlusive lesion score (mAOL) on follow-up CTA with mAOL of 3 representing good recanalization and final infarct volume (FIV), determined in an automated fashion (Boers et al., 2013).

2.7. Statistical analysis

The distribution of the five TAI measures, baseline and outcome clinical variables are presented using mean and standard deviation (SD) if normally distributed or with median and interquartile range (IQR) otherwise. Normality of the distributions was assessed using the Shapiro-Wilk test. Categorical and ordinal data were presented using count and proportions. TAI outliers were eliminated using the Tukey outlier filter method (Hoaglin et al., 1986). Differences between the five TAI distributions were assessed using pairwise comparisons (the Student test or the Wilcoxon signed-rank test). The associations of the 5 TAI measures with categorical outcomes were assessed by performing univariate regressions analysis and the calculation of the area under the receiver operating characteristic curve (AUC). Odds ratios (OR) with 95% confidence intervals (95 %CI) for primary and secondary outcome were calculated per 10 HU increase. Significances of differences between the various TAI measures were assessed using the paired Wilcoxon *t*-test for both with primary and secondary outcome groups.

Multivariable logistic regression analysis with all baseline characteristics associated with the primary outcome was performed to determine adjusted ORs. Associations of baseline variables with primary and secondary outcomes were evaluated using univariate logistic regression to select variables to be included in the multivariable models.

Baseline clinical variables significantly associated with an outcome measure were associated to TAIs using one-way Kruskal–Wallis ANOVA for ordinal variables. The Spearman's correlation coefficient was calculated for non-normal distributed variables, or the Pearson's correlation coefficient for normally distributed variables. The Wilcoxon

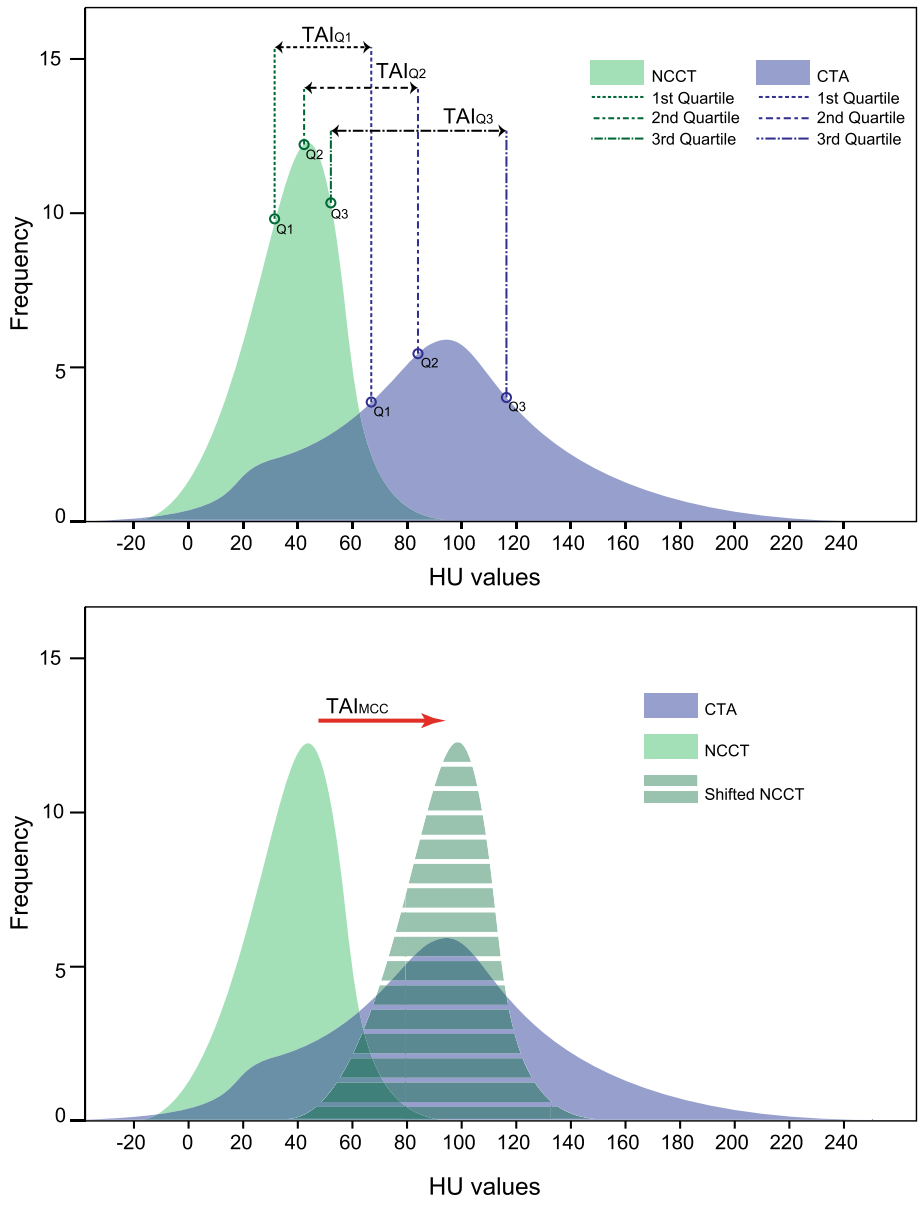

Fig. 2. Example graph of a thrombus attenuation histogram of on CTA and on NCCT image, its 1st, 2nd, 3rd quartiles, MCC. HU indicates Hounsfield Unit; CTA, computed tomography angiography; NCCT, non-contrast computed tomography; TAI, thrombus attenuation increase; Q1, 1st Quartile; Q2, 2nd Quartile; and Q3, 3rd Quartile; and MCC, Maximum lag of the Cross Correlation of the entire thrombus density distribution.

signed-rank test was used for dichotomized data. Baseline clinical variables with significant association with functional outcome measures were included in subsequent multivariable logistic regression models. Optimal model selection was performed by comparison of the Akaike information criterion (AIC) and Bayesian information criterion (BIC).

Associations of the five TAI measures with FIV were studied using univariate linear regressions. To measure the degree of linear dependence of the TAI measure with FIV, the Pearson's coefficient was calculated for normally distributed variables, and the Spearman's correlation coefficient otherwise. The linear regression models were compared using AIC and BIC.

Significance level was set to p-value of 0.05. All analyses were performed using IBM SPSS Statistics software, version 21.0 (IBM Corporation, Armonk, NY, USA).

3. Results

The average age of our study group was 65 (±12) years, 62% (118) of the patients were male and the median admission National Institutes of Health Stroke Scale (NHISS) was 18(±6). The majority (53%) of the patients had an unfavorable functional outcome. All baseline and outcome characteristics, their descriptive analysis, and their associations with TAI and favorable outcome are presented in Supplemental Table 1. In summary, patients with favorable functional outcome were younger, had lower NIHSS. Patients who were successfully treated and treated with endovascular treatment had better functional outcome. The associations with recanalization, separated per treatment group, is presented in the Supplemental Table 2.

Twenty (11%) patients required additional manual correction of the image registration and using Tukey's method, 6 patients were outliers. Median TAIs were 11 (IQR: 1–23) HU, 7(IQR: 0–11) HU, 7 (2–14) HU, 9 (3–18) HU, and 8(IQR: 1–12) HU respectively for the Manual, the Q1, the Q2, the Q3 and the MCC lag measure.

Table 1
Association of TAI measures to with outcomes using logistic regression analysis receiver operating curve analysis, linear regression and Akaike and Bayesian information criterion.

Functional Outcome (n = 189)									
		Favorable	**Unfavorable**	**MW**	**Univariate analysis**		**ROC analysis**	**Information criteria**	
	Median (IQR)	Median (IQR)		P	OR (95 %CI)	p	AUC (95 %CI)	AIC	BIC
TAIobs	11(1–23)	15(5–29)	8(0–19)	0.023*	1.15(1.00–1.32)	0.055	0.60(0.51–0.68)	237.5	244
TAIQ1	7(0–11)	8(3–14)	6(0–10)	0.011*	1.63(1.19–2.25)	0.003*	0.61(0.53–0.69)	230.4	236.9
TAIQ2	7(2–14)	10(4–17)	6(1–10)	0.005*	1.56(1.16–2.10)	0.003*	0.62(0.54–0.70)	235.9	242.4
TAIQ3	9(3–18)	11(5–20)	7(2–17)	0.023*	1.24(1.00–1.54)	0.045*	0.60(0.51–0.68)	238.5	245
MCC	8(1–12)	9(4–16)	5(1–11)	0.001*	1.70(1.24–2.34)	0.001*	0.64(0.56–0.72)	103.9	110.4
Recanalization (n = 148)									
Control									
		Complete	**No or incomplete**	**MW**	**Univariate analysis**		**ROC analysis**	**Information criteria**	
	Median (IQR)	Median (IQR)		P	OR (95 %CI)	p	AUC (95 %CI)	AIC	BIC
TAIobs	12(4–27)	19.4(6.1–32.9)	11.2(-0.9–18.4)	0.083	1.20(0.98–1.47)	0.081	0.61(0.49–0.73)	114.2	119.3
TAIQ1	7(0–11)	8.4(4.8–13.9)	4(-0.1–9.3)	0.026*	1.73(1.08–2.76)	0.023*	0.64(0.52–0.75)	111.8	116.9
TAIQ2	7(2–14)	9.7(6.2–15.4)	6.2(0.3–12.9)	0.019*	1.78(1.12–2.82)	0.015*	0.65(0.53–0.76)	115.7	120.8
TAIQ3	9(3–18)	12.2(6.8–20.6)	6.3(0.8–15.9)	0.017*	1.39(1.00–1.92)	0.047*	0.65(0.54–0.76)	116.9	122
MCC	7(2–13)	10.0(6.0–13.5)	5.0(0–11.0)	0.018*	1.67(1.05–2.65)	0.029*	0.65(0.53–0.76)	70.2	75.2
Intra-arterial treatment									
	IAT	**Complete**	**No or incomplete**	**MW**	**Univariate analysis**		**ROC analysis**	**Information criteria**	
	Median (IQR)	Median (IQR)		P	OR (95 %CI)	p	AUC (95 %CI)	AIC	BIC
TAIobs	15(2–24)	17(3–30)	9(0–18)	0.17	1.40(0.92–2.13)	0.12	0.63(0.47–0.79)	55.7	59.7
TAIQ1	7(3–13)	7(3–13)	6(2–14)	0.74	1.14(0.52–2.51)	0.75	0.53(0.33–0.73)	58.8	62.8
TAIQ2	8(2–15)	8(2–14)	11(2–17)	0.58	0.92(0.48–1.76)	0.80	0.45(0.25–0.64)	61.6	65.7
TAIQ3	9(3–20)	8(3–19)	16(5–27)	0.33	0.81(0.50–1.30)	0.37	0.41(0.21–0.60)	59.5	63.6
MCC	8(1–14)	8(1–12)	13(1–16)	0.43	0.82(0.42–1.57)	0.54	0.42(0.22–0.63)	52.2	56.2

3.1. Primary outcome: Functional outcome

All TAI measures were significantly different between patients with favorable and unfavorable functional outcome. The distributions of the measured TAI per outcomes and per treatment group are shown in Fig. 3. In the univariate models, the ORs (95% CI, p) for a favorable outcome per 10HU increase in TAIs were 1.63(95 %CI:1.19–2.25, p = 0.003) for Q1, 1.56(95 %CI:1.16–2.10, p = 0.003) for Q2, 1.24(95 % CI:1.00–1.54, p = 0.045) for Q3 and 1.70(95 %CI:1.24–2.34, p = 0.001) for MCC. The association between TAI_{manual} and favorable outcome was not statistically significant with an OR of 1.15(95 %CI: 1.00–1.32, p = 0.055). The AUCs of the ROC curves were 0.60, 0.61, 0.62, 0.60 and 0.64 respectively for the TAI_{Manual}, TAIQ1, TAIQ2, TAIQ3 and TAIMCC. The AIC and BIC were both lowest for the mode including TAI derived from the MCC (Table 1).

3.2. Secondary outcome: recanalization status and final infarct volume

One hundred and forty-eight patients had recanalization status available. Amongst the 93 patients in the control group all the entire thrombus TAI measures were significantly different between patients with and without complete recanalization. However, the manual TAI measure was not (p = 0.083). In the univariate models, the ORs (95% CI, p) for a complete recanalization per 10HU increase in TAIs ranged from 1.39 (95 %CI: 1.00–1.92, p = 0.047) for Q3 to 1.78 (95 %CI: 1.12–2.82, p = 0.015) for Q2. There was no significant association (p = 0.055) between TAI_{Manual} and complete recanalization. The AUCs of the ROC curves ranged from 0.61 to 0.65 respectively for TAI_{Manual} and TAIQ2, TAIQ3 and TAIMCC. AIC and BIC were both lowest for TAI for the model including the MCC derived measure. In the IAT group none of the TAI measures were significantly different per recanalization status (Table 1). All TAI measures were significantly associated with FIV with Spearman's correlation coefficients ranging from −0.21 (p = 0.01) for Q1 to −0.31(p < 0.001) for Q3 (Table 2).

3.3. Multivariable analysis

Amongst clinical variables, only age and baseline NIHSS were significantly associated with favorable outcome (p = 0.003, and p = 0.002 respectively). Only baseline NIHSS was significantly correlated with TAIQ1 (Table 2). NIHSS, age and corresponding interaction terms were added in all models. In the multivariable models, TAI_{Q1}, TAI_{Q2} and TAI_{MCC} were independently associated with favorable functional outcome. AIC and BIC were the lowest for TAI_{MCC} (Table 3).

Table 2
Association of TAI measures with continuous baseline and final infarct volume using linear regression, Pearson and Spearman correlation coefficients, and Akaike and Bayesian information criterion

	Pearson (p)		**Spearman (p)**	**AIC**	**BIC**
	Baseline variables		**Follow-up variable**		
TAI	**Age**	**NIHSS**	**FIV**		
Manual	−0.11(0.13)	−0.12(0.09)	**−0.27 (0.001)***	1337.4	1343.3
Q1	0.04(0.57)	**−0.15(0.04)***	**−0.21 (0.01)***	1339.9	1345.9
Q2	0.01(0.84)	−0.14(0.05)	**−0.30 (<0.001)***	1335.7	1341.7
Q3	−0.02(0.82)	−0.13(0.08)	**−0.31 (<0.001)***	1337.1	1343.0
MCC	−0.02(0.80)	−0.13(0.08)	**−0.28 (0.001)***	1336.6	1342.5

TAI indicates thrombus attenuation increase; FIV, final infract volume; NHISS, National institutes of health stroke scale; CI, confidence interval; Q1, 1st Quartile; Q2, 2nd Quartile; and Q3, 3rd Quartile of the entire thrombus density distribution; MCC, Maximum lag of the Cross Correlation of the entire thrombus density distribution; AIC, Akaike information criterion; BIC, Bayesian information criterion; p, significance value;
*, p is significant at the 0.05 level.

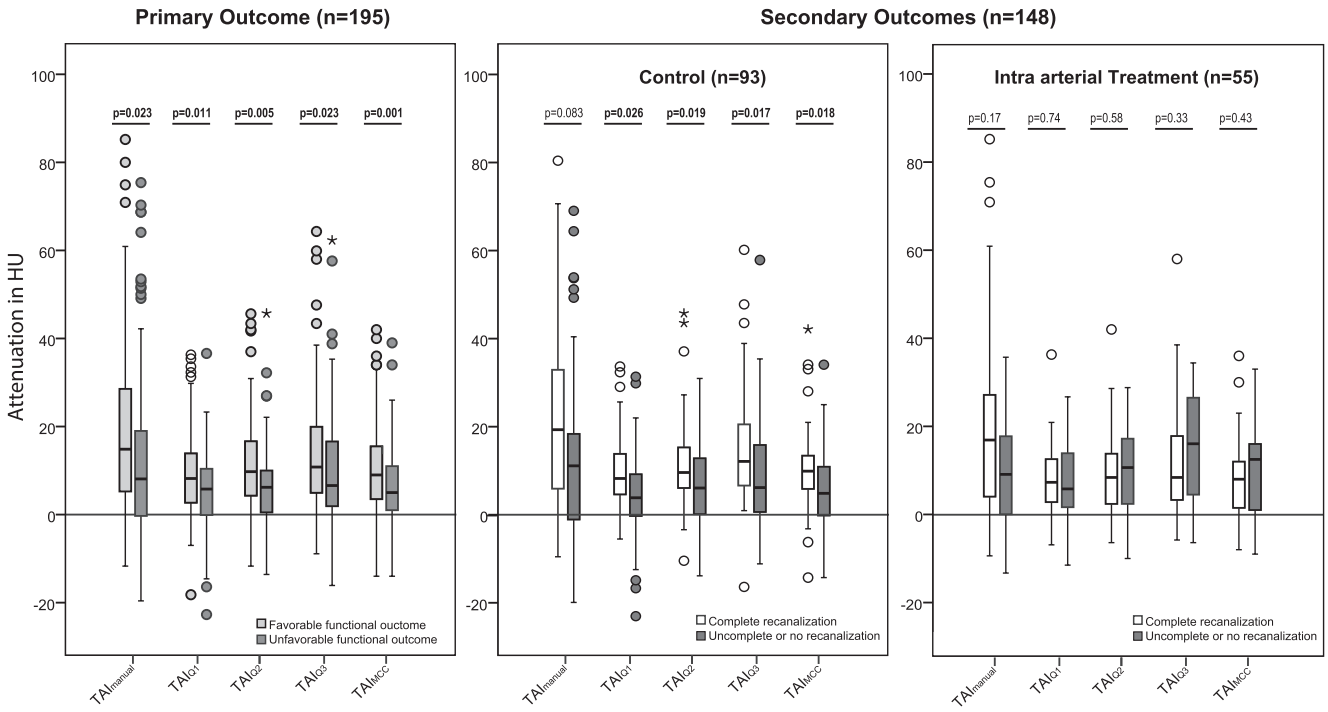

Fig. 3. Boxplot of the 5 TAI measures for favorable and unfavorable outcome and for recanalization for the Control group and the Intra-arterial treatment group (complete recanalization (mAOL=3) or incomplete or partial recanalization (mAOL<3)). HU indicates Hounsfield Unit; mRS, modified Rankin Scale; mAOL, modified arterial occlusive lesion score; Q1, 1st Quartile; Q2, 2nd Quartile; and Q3, 3rd Quartile; MCC, Maximum of the Cross Correlation.

Table 3
Association of TAI measures with favorable functional outcome (mRS $\leq$ 2) using multivariable logistic regression analysis, Akaike and Bayesian information criterion

TAI	aOR(95 %CI,p)	AIC	BIC
Manual	1.10(0.94–1.28),0.22	235.6	248.5
Q1ǂ	**1.65(1.15–2.38),0.01***	229.0	242.0
Q2	**1.55(1.11–2.16),0.01***	229.8	242.8
Q3	1.21(0.96–1.54),0.11	234.5	247.5
MCC	**1.73(1.22–2.47),0.002***	226.7	239.7

TAI indicates thrombus attenuation increase; aOR, adjusted odds ratio; CI, confidence interval; Q1, 1st Quartile; Q2, 2nd Quartile; and Q3, 3rd Quartile of the entire thrombus density distribution; MCC, Maximum lag of the Cross Correlation of the entire thrombus density distribution; NIHSS, National institutes of health stroke scale; AIC, Akaike information criterion; BIC, Bayesian information criterion; p, significance value; mRS, modified Rankin Scale. mRS score: 0, no symptoms at all; 1, no significant disability despite symptoms; 2, slight disability; 3, moderate disability; 4, moderately severe disability; 5, severe disability; 6, dead.
*, p is significant at the 0.05 level. ǂ Model include an interaction term Q1*NIHSS.

4. Discussion

This study shows that, compared to TAI derived from manually selected regions, novel TAI measures derived from full thrombus segmentation are more strongly associated with functional outcome, as well as with follow-up recanalization in patients receiving best medical treatment with intravenous alteplase if eligible. The TAI MCC lags and Q2 values derived from entire thrombus segmentations were the only independent predictors of final outcome in the multivariate models including NIHSS, age and recanalization status. For the secondary outcome measure FIV, all TAI measures were associated, with little difference in effect size.

The lowest AIC and BIC and highest association with favorable outcome and recanalization was found for the cross correlation of CTA and NCCT densities distributions derived over the entire thrombus. Thrombi are heterogeneous(Singh et al., 2013) and have shown to have very variable CT attenuation distributions (Santos et al., 2016c). In our study, we have used single values to describe the TAI distribution values, such as quartiles or mean, for the entire thrombus. This is an over-simplification of the distribution complexity and may thereby have reduced its predictive value. This may explain the better performance of the cross-correlation feature.

In a previous study, the manual TAI measure was significantly associated with functional outcome (Santos et al., 2016b). However, in the current study, the association of the continuous manual TAI measure with functional outcome was not statistically significant. The previous study on the MRCLEAN database used dichotomized perviousness, in which the threshold was optimized to maximize sensitivity and specificity, reflected in the stronger association with functional outcome.

It was previously shown that observers tend to measure the attenuation at denser parts of thrombi on NCCT (Santos et al., 2016c). In our study, manual TAI values were overall higher than TAI values derived from entire thrombi. This implies that high-density thrombus parts on NCCT also showed a higher increase in attenuation on CTA, which may suggest that high-density thrombi are more pervious. This is in line with previous studies showing that high-density thrombi are more responsive to IV-rtPA and showing that IV-rtPA is more successful in pervious thrombi (Bilgic et al., 2020; Dutra et al., 2019; Kappelhof et al., 2018; Niesten et al., 2014; Santos et al., 2016a). The higher manual TAI value might also arise from partial volume effect. Since the edges of the thrombus are included in the entire TAI measurements, it is expected that the automated TAI values are somewhat lower, in particularly for small thrombi. However, this effect has been previously evaluated on $\leq$2.5 mm slice data and neither the volume of the thrombus nor the slice thickness reconstruction of the NCCT images were associated with the measured median thrombus density values (Santos et al., 2016e).

This study has limitations. We chose to use continuous TAI for assessment of associations with outcome and have not applied a threshold value to dichotomize thrombi as pervious or impervious as in previous studies (Berndt et al., 2018; Santos et al., 2016b, 2016a). Direct

comparison of associations of continuous versus dichotomized TAI is not straight-forward because optimal threshold value differs with imaging protocol and patient cohort (Berndt et al., 2018; Kappelhof et al., 2018; Mokin et al., 2020; Santos et al., 2016b, 2016a). This might explain that, in contrary to the Dutch Acute Stroke Study (DUST) population study, we did not find a significant association between manual assessments of TAI with complete recanalization in our Control group (Santos et al., 2016a). However, the association with recanalization was significant for all entire-thrombus TAI measures.

A third study reported no clear association between TAI and stroke subtype (Boodt et al., 2020).

Possible mechanisms and characteristics responsible for the contrast penetrating a thrombus (e.g. permeability, local pressure, composition, retraction, length, and location) and their clinical impact (e.g. admission deficit, IV-rtPA efficacy, functional outcome, and antegrade flow) in patients with an acute ischemic stroke still need further investigation. Our results suggest that the study of these mechanisms would be improved when considering entire thrombus imaging characteristics. Entire thrombus delineations by an observer is tedious. A few computer assisted methods ranging from simple (Ahn and Kim, 2012; Nam et al., 2012) to more advanced (Santos et al., 2014) have been proposed to support that task. With the growing interest in the use of reliable biomarkers for prediction of acute ischemic stroke treatment outcome, it is clear that segmentation tools - such as the one presented in this study – will be valuable, in particular to the use of thrombus characteristics in acute stroke management (Menon et al., 2018; Dutra et al., 2019; Niesten et al., 2013; Riedel et al., 2011; Shobha et al., 2013).

5. Conclusion

Thrombus perviousness measures from entire thrombus segmentation have a significantly stronger association with functional outcome and recanalization after intravenous alteplase compared to current manual assessments using regions of interests. The lag of the cross correlation of the entire thrombus intensity distributions on CTA and NCCT was the strongest associated with both functional outcome and recanalization after intravenous alteplase. Tools for entire thrombus segmentation may support further development of the use of these measures in stroke research and clinical practice.

6. Sources of funding

This study has been funded by the Technology Foundation STW under Grant 11632, http://www.carisma-airspace.nl, ITEA2 project MEDUSA under grant number 10004, https://itea3.org/project/medusa.html, and the European Union Horizon 2020 research and innovation program under grant number 777072, https://www.insist-h2020.eu/.

The MR CLEAN trial was funded by the Dutch Heart Foundation and through unrestricted grants from AngioCare BV, Covidien/EV3®, MEDAC Gmbh/LAMEPRO and Penumbra Inc.

The MR CLEAN Investigators

Executive committee

Diederik W.J. Dippel[1]; Aad van der Lugt[2]; Charles B.L.M. Majoie[3]; Yvo B.W.E.M. Roos[4]; Robert J. van Oostenbrugge[5]; Wim H. van Zwam[6]; Olvert A. Berkhemer[1,3]; Puck S.S. Fransen[1,2]; Debbie Beumer[1,5]; Lucie A. van den Berg[4]

Local principal investigators

Wouter J. Schonewille[7]; Jan Albert Vos[8]; Charles B.L.M. Majoie[3]; Yvo B.W.E.M. Roos[4]; Paul J. Nederkoorn[4]; Marieke J.H. Wermer[9]; Marianne A.A. van Walderveen[10]; Robert J. van Oostenbrugge[5]; Wim H. van Zwam[6]; Julie Staals[5]; Jeannette Hofmeijer[11]; Jacques A. van Oostayen[12]; Geert J. Lycklama à Nijeholt[13]; Jelis Boiten[14]; Diederik W.J. Dippel[1]; Patrick A. Brouwer[2]; Bart J. Emmer[2]; Sebastiaan F. de Bruijn[15]; Lukas C. van Dijk[16]; L. Jaap Kappelle[17]; Rob H. Lo[18]; Ewoud J. van Dijk[19]; Joost de Vries[20]; Paul L.M. de Kort[21]; Jan S.P. van den Berg[22]; Boudewijn A.A.M. van Hasselt[23]; Leo A.M. Aerden[24]; René J. Dallinga[25]; Marieke C. Visser[26]; Joseph C.J. Bot[27]; Patrick C. Vroomen[28]; Omid Eshghi[29]; Tobien H.C.M.L. Schreuder[30]; Roel J.J. Heijboer[31]; Koos Keizer[32]; Alexander V. Tielbeek[33]; Heleen M. den Hertog[34]; Dick G. Gerrits[35]; Renske M. van den Berg-Vos[36]; Giorgos B. Karas[37]

Imaging assessment committee

Charles B.L.M. Majoie[3] (chair); Wim H. van Zwam[6]; Aad van der Lugt[2]; Geert J. Lycklama à Nijeholt[13]; Marianne A.A. van Walderveen[10], Joseph C.J. Bot[27]; Henk A. Marquering[38]; Ludo F. Beenen[3]; Marieke E.S. Sprengers[3]; Sjoerd F.M. Jenniskens[39], René van den Berg[3]; Olvert A. Berkhemer[1,3]; Albert J. Yoo[40]

Outcome assessment committee

Yvo B.W.E.M. Roos[4] (chair); Peter J. Koudstaal[1]; Jelis Boiten; Ewoud J. van Dijk[19]

Adverse event committee

Robert J. van Oostenbrugge[5] (chair); Marieke J.H. Wermer[9]; H. Zwenneke Flach[23]

Trial statisticians

Ewout W. Steyerberg[41]; Hester F. Lingsma[41]

Data monitoring committee

Martin M. Brown[42] (Chair); Thomas Liebig[43]; Theo Stijnen[44]; Hester F. Lingsma[41]

Advisory board:

Tommy Andersson[45]; Heinrich P. Mattle[46]; Nils Wahlgren[47]; Peter J. Koudstaal[1]

Research nurses / local trial coordinators

Esther van der Heijden[1]; Naziha Ghannouti[1]; Nadine Fleitour[4]; Imke Hooijenga[4]; Annemieke Lindl-Velema[5]; Corina Puppels[7]; Wilma Pellikaan[7]; Kirsten Janssen[9]; Nicole Aaldering[11]; Marjan Elfrink[11]; Joke de Meris[14]; Annet Geerlings[19]; Gina van Vemde[22]; Ans de Ridder[17]; Paut Greebe[17]; José de Bont-Stikkelbroeck[21]; Willy Struijk[15]; Tiny Simons[30]; Gert Messchendorp[28]; Friedus van der Minne[28]; Hester Bongenaar[32]; Karin Bodde[26];

PhD / Medical students:

Silvan Licher[1]; Nikki Boodt; Adriaan Ros[1]; Esmee Venema[1]; Ilse Slokkers[1]; Raymie-Jayce Ganpat[1]; Maxim Mulder[1]; Nawid Saiedie[1]; Alis Heshmatollah[1]; Stefanie Schipperen[1]; Stefan Vinken[1]; Tiemen van Boxtel[1]; Jeroen Koets[1]; Merel Boers[38]; Emilie Santos[2; 38]; Jordi Borst[3]; Ivo Jansen[3]; Manon Kappelhof[3]; Marit Lucas[38]; Ralph Geuskens[38]; Renan Sales Barros[38]; Roeland Dobbe[38]; Marloes Csizmadia[38]

List of affiliations

Department of Neurology[1], Radiology[2], Public Health[41], Erasmus MC University Medical Center; Department of Radiology[3], Neurology[4], Biomedical Engineering and Physics[38], Academic Medical Center,

Amsterdam; Department of Neurology[5], Radiology[6], Maastricht University Medical Center and Cardiovascular Research Institute Maastricht (CARIM); Department of Neurology[7], Radiology[8], Sint Antonius Hospital, Nieuwegein; Department of Neurology[9], Radiology[10], Medical Statistics and Bioinformatics[44], Leiden University Medical Center; Department of Neurology[11], Radiology[12], Rijnstate Hospital, Arnhem; Department of Radiology[13], Neurology[14], MC Haaglanden, the Hague; Department of Neurology[15], Radiology[16], HAGA Hospital, the Hague; Department of Neurology[17], Radiology[18], University Medical Center Utrecht; Department of Neurology[19], Neurosurgery[20], Radiology[39], Radboud University Medical Center, Nijmegen; Department of Neurology[21], Sint Elisabeth Hospital, Tilburg; Department of Neurology[22], Radiology[23], Isala Klinieken, Zwolle; Department of Neurology[24], Radiology[25], Reinier de Graaf Gasthuis, Delft; Department of Neurology[26], Radiology[27], VU Medical Center, Amsterdam; Department of Neurology[28], Radiology[29], University Medical Center Groningen, the Netherlands; Department of Neurology[30], Radiology[31], Atrium Medical Center, Heerlen; Department of Neurology[32], Radiology[33], Catharina Hospital, Eindhoven; Department of Neurology[34], Radiology35, Medical Spectrum Twente, Enschede; Department of Neurology[36], Radiology[37], Sint Lucas Andreas Hospital, Amsterdam; all in the Netherlands; Department of Radiology[40], Texas Stroke Institute, Texas, United States of America; UCL Institute of Neurology[42], National Hospital for Neurology and Neurosurgery, London, United Kingdom; Med. Fakultät[43], Uniklinik Köln, Germany; Department of Radiology[45], Neurology[47], Karolinska Univeristy Hospital, Stockholm, Sweden; Department of Neurology[46], University Hospital of Bern, Switzerland

7. Declaration of Competing Interest

This study has been funded by the Technology Foundation STW under Grant 11632, http://www.carisma-airspace.nl, ITEA2 project MEDUSA under grant number 10004, https://itea3.org/project/medusa.html, and the European Union Horizon 2020 research and innovation program under grant number 777072, https://www.insist-h2020.eu/.

The MR CLEAN trial was funded by the Dutch Heart Foundation and through unrestricted grants from AngioCare BV, Covidien/EV3®, MEDAC Gmbh/LAMEPRO and Penumbra Inc.

Prof. Niessen is co-founder and shareholder of Quantib BV; Dr Marquering and Dr Boers are co-founder and shareholder of Nico-lab BV; The Academic Medical Center Amsterdam received payment from Stryker Inc. for consultations by Prof. Majoie, Erasmus MC received payment from Stryker Inc. for consultations by Prof. Dippel. The other authors report no conflicts. The funders had no role in study design, data collection and analysis, decision to publish, or preparation of the manuscript.

Declaration of Competing Interest

The authors declare that they have no known competing financial interests or personal relationships that could have appeared to influence the work reported in this paper.

Acknowledgements

We are grateful to Mark D. den Blanken for his imaging assessment support.

Appendix A. Supplementary material

Supplementary data to this article can be found online at https://doi.org/10.1016/j.jbiomech.2021.110700.

References

Ahn, S.H., d'Esterre, C.D., Qazi, E.M., Najm, M., Rubiera, M., Fainardi, E., Hill, M.D., Goyal, M., Demchuk, A.M., Lee, T.Y., Menon, B.K., 2015. Occult anterograde flow is an under-recognized but crucial predictor of early recanalization with intravenous tissue-type plasminogen activator. Stroke 46 (4), 968–975. https://doi.org/10.1161/STROKEAHA.114.008648.

Ahn, S.S., Kim, E.Y., 2012. Thrombus imaging in acute ischaemic stroke using thin-slice unenhanced CT: comparison of conventional sequential CT and helical CT. Eur. Radiol. 22 (11), 2392–2396. https://doi.org/10.1007/s00330-012-2518-y.

Arrarte Terreros, N., Tolhuisen, M.L., Bennink, E., de Jong, H.W.A.M., Beenen, L.F.M., Majoie, C.B.L.M., van Bavel, E.d., Marquering, H.A., 2020. From perviousness to permeability, modelling and measuring intra-thrombus flow in acute ischemic stroke. J. Biomech. 111, 110001. https://doi.org/10.1016/j.jbiomech.2020.110001.

Bembenek, J.P., Niewada, M., Siudut, J., Plens, K., Członkowska, A., Undas, A., 2017. Fibrin clot characteristics in acute ischaemic stroke patients treated with thrombolysis: the impact on clinical outcome. Thromb. Haemost. 117 (07), 1440–1447. https://doi.org/10.1160/TH16-12-0954.

Benson, J.C., Fitzgerald, S.T., Kadirvel, R., Johnson, C., Dai, D., Karen, D., Kallmes, D.F., Brinjikji, W., 2020. Clot permeability and histopathology: is a clot's perviousness on CT imaging associated with histologic composition? J. Neurointerv. Surg. 12, 38–42.

Berkhemer, O.A., Fransen, P.S.S., Beumer, D., Van Den Berg, L.A., Lingsma, H.F., Yoo, A. J., 2015. A randomized trial of intraarterial treatment for acute ischemic stroke. N. Engl. J. Med. 372, 11–20. https://doi.org/10.1016/j.jemermed.2015.02.026.

Berndt, M., Friedrich, B., Maegerlein, C., Moench, S., Hedderich, D., Lehm, M., Zimmer, C., Straeter, A., Poppert, H., Wunderlich, S., Schirmer, L., Oberdieck, P., Kaesmacher, J., Boeckh-Behrens, T., 2018. Thrombus permeability in admission computed tomographic imaging indicates stroke pathogenesis based on thrombus histology. Stroke 49 (11), 2674–2682. https://doi.org/10.1161/STROKEAHA.118.021873.

Menon, B.K., Al-Ajlan, F.S., Najm, M., Puig, J., Castellanos, M., Dowlatshahi, D., Calleja, A., Sohn, S.-I., Ahn, S.H., Poppe, A., Mikulik, R., Asdaghi, N., Field, T.S., Jin, A., Asil, T., Boulanger, J.-M., Smith, E.E., Coutts, S.B., Barber, P.A., Bal, S., Subramanian, S., Mishra, S., Trivedi, A., Dey, S., Eesa, M., Sajobi, T., Goyal, M., Hill, M.D., Demchuk, A.M., 2018. Association of clinical, imaging, and thrombus characteristics with recanalization of visible intracranial occlusion in patients with acute ischemic stroke. JAMA 320 (10), 1017. https://doi.org/10.1001/jama.2018.12498.

Bilgic, A.B., Gocmen, R., Arsava, E.M., Topcuoglu, M.A., 2020. The effect of clot volume and permeability on response to intravenous tissue plasminogen activator in acute ischemic stroke. J. Stroke Cerebrovasc. Dis. 29 (2), 104541. https://doi.org/10.1016/j.jstrokecerebrovasdis.2019.104541.

Boers, A.M., Marquering, H.A., Jochem, J.J., Besselink, N.J., Berkhemer, O.A., van der Lugt, A., Beenen, L.F., Majoie, C.B., 2013. Automated cerebral infarct volume measurement in follow-up noncontrast CT scans of patients with acute ischemic stroke. AJNR. Am. J. Neuroradiol. 34 (8), 1522–1527. https://doi.org/10.3174/ajnr.A3463.

Boodt, N., Compagne, K.C.J., Dutra, B.G., Samuels, N., Tolhuisen, M.L., Alves, H.C.B.R., Kappelhof, M., Lycklama à Nijeholt, G.J., Marquering, H.A., Majoie, C.B.L.M., Lingsma, H.F., Dippel, D.W.J., van der Lugt, A., Roos, Y., van Oostenbrugge, R., van Zwam, W., Boiten, J., Vos, J.A., Jansen, I., Mulder, M., Goldhoorn, R.-J., Schonewille, W., Vos, J.A., Coutinho, J., Wermer, M., van Walderveen, M., Staals, J., van Zwam, W., Hofmeijer, J., Martens, J., Boiten, J., Roozenbeek, B., Emmer, B., de Bruijn, S., van Dijk, L., van der Worp, H.B., Lo, R., van Dijk, E., Boogaarts, H., de Kort, P., van Tuijl, J., Peluso, J.o., van den Berg, J., van Hasselt, B., Aerden, L., Dallinga, R., Uyttenboogaart, M., Eshghi, O., Bokkers, R., Schreuder, T., Heijboer, R., Keizer, K., Yo, L., den Hertog, H., Sturm, E., van Zwam, W., van Walderveen, M., Sprengers, M., Jenniskens, S., van den Berg, R., Yoo, A., Beenen, L., Postma, A., Roosendaal, S., van der Kallen, B., van den Wijngaard, I., van Es, A., Emmer, B., Martens, J., Yo, L., Vos, J.A., Bot, J., van Doormaal, P.-J., Roos, Y., van Oostenbrugge, R., van Zwam, W., Boiten, J., Vos, J.A., Schonewille, W., Hofmeijer, J., van der Worp, B., Lo, R., van Oostenbrugge, R., Hofmeijer, J., Flach, Z., el Ghannouti, N., Sterrenberg, M., Puppels, C., Pellikaan, W., Sprengers, R., Elfrink, M., de Meris, J., Vermeulen, T., Geerlings, A., van Vemde, G., Simons, T., van Rijswijk, C., Bongenaar, H., Bodde, K., Kleijn, S., Lodico, J., Droste, H., Wollaert, M., Jeurrissen, D., Bos, E., Drabbe, Y., Zweedijk, B., Khalilzada, M., Venema, E., Chalos, V., Geuskens, R., van Straaten, T., Ergezen, S., Harmsma, R., Muijres, D., de Jong, A., Hinseveld, W., Berkhemer, O., Boers, A., Huguet, J., Groot, P., Mens, M., van Kranendonk, K., Treurniet, K., Tolhuijsen, M., 2020. Stroke etiology and thrombus computed tomography characteristics in patients with acute ischemic stroke: a MR CLEAN registry substudy. Stroke 51 (6), 1727–1735. https://doi.org/10.1161/STROKEAHA.119.027749.

Borst, J., Berkhemer, O.A., Santos, E.M.M., Yoo, A.J., den Blanken, M., Roos, Y.B.W.E.M., van Bavel, E., van Zwam, W.H., van Oostenbrugge, R.J., Lingsma, H.F., van der Lugt, A., Dippel, D.W.J., Marquering, H.A., Majoie, C.B.L.M., 2017. Value of thrombus CT characteristics in patients with acute ischemic stroke. Am. J. Neuroradiol. 38 (9), 1758–1764. https://doi.org/10.3174/ajnr.A5331.

Dutra, B.G., Tolhuisen, M.L., Alves, H.C.B.R., Treurniet, K.M., Kappelhof, M., Yoo, A.J., Jansen, I.G.H., Dippel, D.W.J., van Zwam, W.H., van Oostenbrugge, R.J., da Rocha, A.J., Lingsma, H.F., van der Lugt, A., Roos, Y.B.W.E.M., Marquering, H.A., Majoie, C.B.L.M., 2019. Thrombus imaging characteristics and outcomes in acute ischemic stroke patients undergoing endovascular treatment. Stroke 50 (8), 2057–2064. https://doi.org/10.1161/STROKEAHA.118.024247.

Fereidoonnezhad, B., Dwivedi, A., Johnson, S., Mccarthy, R., Mcgarry, P., 2020. Blood clot fracture properties are dependent on red blood cell and fibrin content. Acta Biomater. (under Rev.).

Frölich, A.M.J., Psychogios, M.N., Klotz, E., Schramm, R., Knauth, M., Schramm, P., 2012. Antegrade flow across incomplete vessel occlusions can be distinguished from retrograde collateral flow using 4-dimensional computed tomographic angiography. Stroke 43 (11), 2974–2979. https://doi.org/10.1161/STROKEAHA.112.668889.

Gunning, G.M., McArdle, K., Mirza, M., Duffy, S., Gilvarry, M., Brouwer, P.A., 2018. Clot friction variation with fibrin content; implications for resistance to thrombectomy. J. Neurointerv. Surg. 10 (1), 34–38. https://doi.org/10.1136/neurintsurg-2016-012721.

Heckel, F., Schwier, M., Peitgen, H., n.d. Object-oriented application development with MeVisLab and Python.

Hoaglin, D.C., Iglewicz, B., Tukey, J.W., 1986. Performance of some resistant performance rules for labeling outlier. J. Am. Stat. Assoc. 81, 991–999.

Johnson, S., Chueh, J., Gounis, M.J., McCarthy, R., McGarry, J.P., McHugh, P.E., Gilvarry, M., 2020. Mechanical behavior of in vitro blood clots and the implications for acute ischemic stroke treatment. J. Neurointerv. Surg. 12 (9), 853–857. https://doi.org/10.1136/neurintsurg-2019-015489.

Johnson, S., Duffy, S., Gunning, G., Gilvarry, M., McGarry, J.P., McHugh, P.E., 2017. Review of mechanical testing and modelling of thrombus material for vascular implant and device design. Ann. Biomed. Eng. 45 (11), 2494–2508. https://doi.org/10.1007/s10439-017-1906-5.

Kappelhof, M., Tolhuisen, M.L., Treurniet, K.M., Dutra, B.G., Brown, S., Muir, K.W., Roos, Y.B.W.E.M., Saver, J.L., Demchuk, A.M., Jovin, T.G., Bracard, S., Campbell, B. C.V., Van Der Lugt, A., White, P., Hill, M.D., Dippel, D.W.J., Mitchell, P.J., Goyal, M., Marquering, H.A., Majoie, C.B.L.M., Investigators, O. behalf of the H., 2018. Thrombus perviousness as a potential patient selection tool for intravenous and endovascular treatment for acute ischemic stroke, in: European Stroke Journal. SAGE, Göthenborg, p. 76. doi:10.1177/2396987318770127.

Klein, S., Staring, M., Murphy, K., Viergever, M.A., Pluim, J., 2010. elastix: a toolbox for intensity-based medical image registration. IEEE Trans. Med. Imaging 29 (1), 196–205.

Kufner, A., Erdur, H., Endres, M., Nolte, C.H., Scheel, M., Schlemm, L., 2020. Association between thrombus perviousness assessed on computed tomography and stroke cause. Stroke 51 (12), 3613–3622. https://doi.org/10.1161/STROKEAHA.120.031148.

Labiche, L.A., Malkoff, M., Alexandrov, A.V., 2003. Residual flow signals predict complete recanalization in stroke patients treated with TPA. J. Neuroimaging 13, 28–33. https://doi.org/10.1177/1051228402239714.

Mokin, M., Waqas, M., Fifi, J., De Leacy, R., Fiorella, D., Levy, E.I., Snyder, K., Hanel, R., Woodward, K., Chaudry, I., Rai, A.T., Frei, D., Delgado Almandoz, J.E., Kelly, M., Arthur, A.S., Baxter, B.W., English, J., Linfante, I., Fargen, K.M., Turk, A., Siddiqui, A.H., Mocco, J., 2020. Clot perviousness is associated with first pass success of aspiration thrombectomy in the COMPASS trial. J. Neurointerv. Surg. 13 (6), 509–514. https://doi.org/10.1136/neurintsurg-2020-016434.

Nam, H., Kim, E., Kim, S., Kim, Y., Kim, J., Lee, H., Nam, C., Heo, J., 2012. Prediction of thrombus resolution after intravenous thrombolysis assessed by CT-based thrombus imaging. Thromb. Haemost. 107 (04), 786–794. https://doi.org/10.1160/TH11-08-0585.

Niesten, J.M., van der Schaaf, I.C., Biessels, G.J., van Otterloo, A.E., van Seeters, T., Horsch, A.D., Luitse, M.J.A., van der Graaf, Y., Kappelle, L.J., Mali, W.P.T.M., Velthuis, B.K., 2013. Relationship between thrombus attenuation and different stroke subtypes. Neuroradiology 55 (9), 1071–1079. https://doi.org/10.1007/s00234-013-1217-y.

Niesten, J.M., van der Schaaf, I.C., van der Graaf, Y., Kappelle, L.J., Biessels, G.J., Horsch, A.D., Dankbaar, J.W., Luitse, M.J.A., van Seeters, T., Smit, E.J., Mali, W.P.T. M., Velthuis, B.K., 2014. Predictive value of thrombus attenuation on thin-slice non-contrast CT for persistent occlusion after intravenous thrombolysis. Cerebrovasc. Dis. 37 (2), 116–122. https://doi.org/10.1159/000357420.

Patel, T.R., Fricano, S., Waqas, M., Tso, M., Dmytriw, A.A., Mokin, M., Kolega, J., Tomaszewski, J., Levy, E.I., Davies, J.M., Snyder, K.V., Siddiqui, A.H., Tutino, V.M., 2021. Increased perviousness on CT for acute ischemic stroke is associated with fibrin/platelet-rich clots. Am. J. Neuroradiol. 42 (1), 57–64. https://doi.org/10.3174/ajnr.A6866.

Riedel, C.H., Zimmermann, P., Jensen-Kondering, U., Stingele, R., Deuschl, G., Jansen, O., 2011. The importance of size: Successful recanalization by intravenous thrombolysis in acute anterior stroke depends on thrombus length. Stroke 42 (6), 1775–1777. https://doi.org/10.1161/STROKEAHA.110.609693.

Santos, E.M.M., d'Esterre, C.D., Treurniet, K.M., Niessen, W.J., Najm, M., Goyal, M., Demchuk, A.M., Majoie, C.B., Menon, B.K., Marquering, H.A., Mandzia, J., Fainardi, E., Rubiera, M., Khaw, A.V., Zini, A., Shankar, J.J., 2018. Added value of multiphase CTA imaging for thrombus perviousness assessment. Neuroradiology 60. https://doi.org/10.1007/s00234-017-1907-y.

Santos, E.M.M., Dankbaar, J.W., Treurniet, K.M., Horsch, A.D., Roos, Y.B., Kappelle, L.J., Niessen, W.J., Majoie, C.B., Velthuis, B., Marquering, H.A., Duijm, L.E., Keizer, K., van der Lugt, A., Dippel, D.W., Droogh - de Greeve, K.E., Bienfait, H.P., van Walderveen, M.A., Wermer, M.J., Lycklama à Nijeholt, G.J., Boiten, J., Duyndam, D., Kwa, I.V., Meijer, J.F., van Dijk, E.J., Kesselring, F.O., Hofmeijer, J., Vos, J.A., Schonewille, W.J., van Rooij, W.J., de Kort, P.L., Pleiter, C.C., Bakker, S.L., Bot, J., Visser, M.C., van der Schaaf, I.C., Mali, W.P., van Seeters, T., Niesten, J.M., Biessels, G.J., Luitse, M.J., van der Graaf, Y., 2016a. Permeable thrombi are associated with higher intravenous recombinant tissue-type plasminogen activator treatment success in patients with acute ischemic stroke. Stroke 47 (8), 2058–2065. https://doi.org/10.1161/STROKEAHA.116.013306.

Santos, E.M.M., Marquering, H.A., Berkhemer, O.A., van Zwam, W.H., van der Lugt, A., Majoie, C.B., Niessen, W.J., Baron, J.-C., 2014. Development and validation of intracranial thrombus segmentation on CT angiography in patients with acute ischemic stroke. PLoS One 9 (7), e101985. https://doi.org/10.1371/journal.pone.0101985.

Santos, E.M.M., Marquering, H.A., den Blanken, M.D., Berkhemer, O.A., Boers, A.M.M., Yoo, A.J., Beenen, L.F., Treurniet, K.M., Wismans, C., van Noort, K., Lingsma, H.F., Dippel, D.W.J., van der Lugt, A., van Zwam, W.H., Roos, Y.B.W.E.M., van Oostenbrugge, R.J., Niessen, W.J., Majoie, C.B., Fransen, P.S.S., Beumer, D., van den Berg, L.A., Schonewille, W.J., Vos, J.A., Nederkoorn, P.J., Wermer, M.J.H., van Walderveen, M.A.A., Staals, J., Hofmeijer, J., van Oostayen, J.A., Lycklama à Nijeholt, G.J., Boiten, J., Brouwer, P.A., Emmer, B.J., de Bruijn, S.F., van Dijk, L.C., Kappelle, L.J., Lo, R.H., van Dijk, E.J., de Vries, J., de Kort, P.L.M., van den Berg, J.S. P., van Hasselt, B.A.A.M., Aerden, L.A.M., Dallinga, R.J., Visser, M.C., Bot, J.C.J., Vroomen, P.C., Eshghi, O., Schreuder, T.H.C.M.L., Heijboer, R.J.J., Keizer, K., Tielbeek, A.V., den Hertog, H.M., Gerrits, D.G., van den Berg-Vos, R.M., Karas, G.B., Sprengers, M.E.S., Jenniskens, S.F.M., van den Berg, R., Koudstaal, P.J., Boiten, J., van Dijk, E.J., Wermer, M.J.H., Flach, H.Z., Steyerberg, E.W., Brown, M.M., Liebig, T., Stijnen, T., Andersson, T., Mattle, H.P., Wahlgren, N., Koudstaal, P.J., van der Heijden, E., Ghannouti, N., Fleitour, N., Hooijenga, I., Lindl-Velema, A., Puppels, C., Pellikaan, W., Janssen, K., Aaldering, N., Elfrink, M., de Meris, J., Geerlings, A., van Vemde, G., de Ridder, A., Greebe, P., de Bont-Stikkelbroeck, J., Struijk, W., Simons, T., Messchendorp, G., van der Minne, F., Bongenaar, H., Bodde, K., Licher, S., Boodt, N., Ros, A., Venema, E., Slokkers, I., Ganpat, R.-J., Mulder, M., Saiedie, N., Heshmatollah, A., Schipperen, S., Vinken, S., van Boxtel, T., Koets, J., Boers, M., Borst, J., Jansen, I., Kappelhof, M., Lucas, M., Geuskens, R., Barros, R.S., Dobbe, R., Csizmadia, M., 2016b. Thrombus Permeability is associated with improved functional outcome and recanalization in patients with ischemic stroke. Stroke 47 (3), 732–741. https://doi.org/10.1161/STROKEAHA.115.011187.

Santos, E.M.M., Niessen, W.J., Yoo, A.J., Berkhemer, O.A., Beenen, L.F., Majoie, C.B., Marquering, H.A., Baron, J.-C., 2016c. Automated entire thrombus density measurements for robust and comprehensive thrombus characterization in patients with acute ischemic stroke. PLoS One 11 (1), e0145641. https://doi.org/10.1371/journal.pone.0145641.

Santos, E.M.M., Niessen, W.J., Yoo, A.J., Berkhemer, O.A., Beenen, L.F., Majoie, C.B., Marquering, H.A., 2016d. Automated entire thrombus density measurements for comprehensive characterization of thrombi in patients with acute ischemic stroke. PLoS One.

Santos, E.M.M., Yoo, A.J., Beenen, L.F., Berkhemer, O.A., den Blanken, M.D., Wismans, C., Niessen, W.J., Majoie, C.B., Marquering, H.A., 2016e. Observer variability of absolute and relative thrombus density measurements in patients with acute ischemic stroke. Neuroradiology 58 (2), 133–139. https://doi.org/10.1007/s00234-015-1607-4.

Shobha, N., Bal, S., Boyko, M., Kroshus, E., Menon, B.K., Bhatia, R., Sohn, S.-I., Kumarpillai, G., Kosior, J., Hill, M.D., Demchuk, A.M., 2013. Measurement of length of hyperdense MCA sign in acute ischemic stroke predicts disappearance after IV tPA. J. Neuroimaging 24 (1), 7–10. https://doi.org/10.1111/jon.2014.24.issue-110.1111/j.1552-6569.2012.00761.x.

Singh, P., Kaur, R., Kaur, A., 2013. Clot composition and treatment approach to acute ischemic stroke: The road so far. Ann. Indian Acad. Neurol. 16, 494–497. https://doi.org/10.4103/0972-2327.120433.

Tutwiler, V., Peshkova, A.D., Andrianova, I.A., Khasanova, D.R., Weisel, J.W., Litvinov, R.I., 2017. Contraction of blood clots is impaired in acute ischemic stroke. Arterioscler. Thromb. Vasc. Biol. 37 (2), 271–279. https://doi.org/10.1161/ATVBAHA.116.308622.

WikipediA, 2021. Thrombus perviousness Wikipedia [WWW Document]. Webpage. URL https://en.wikipedia.org/wiki/Thrombus_perviousness (accessed 7.25.21).

Zhang, M., Chen, Z., Xu, J., Gong, X., Shi, F., Lou, M., 2020. Antegrade blood flow on 4-dimensional computed tomography angiography predict stroke subtype in patients with acute large artery occlusion. J. Am. Heart Assoc. 9, e015759 https://doi.org/10.1161/JAHA.119.015759.

Glossary

AIC: Akaike Information Criterion; estimator of prediction error and thereby relative quality of statistical models.
AUC: The area under the receiver operating characteristic curve
BIC: Bayesian Information Criterion; estimator of prediction error and thereby relative quality of statistical models.
CTA: Computed Tomography Angiography
FIV: Final Infarct Volume; the volume of dead brain tissue after acute ischemic stroke.
HU: Hounsfield Unit; Scale for describing radiodensity in CT imaging.
IAT: Intra-Arterial Treatment
IV-rtPA: Intravenously administrated recombinant tissue plasminogen activator. Standard of care for treatment of acute ischemic stroke between 1999 and 2015.
IQR: Interquartile Range
mAOL: Modified Arterial Occlusion Lesion score; a measure of the degree of the opening of an occluded artery after treatment for stroke.
mRS: modified Rankin Scale; a measure for functional outcome in patients with neurological deficits. The mRS ranges from 0 (no symptoms) to 6 (dead).
MCC: Maximum of cross correlation; used to align density distributions of the thrombi in CT images.
mAOL: modified Arterial Occlusive Lesion score; a score to assess the recanalization of the occluded artery in an acute ischemic stroke patient. This measure is commonly performed in follow-up CTA.
MR CLEAN: Multicenter Randomized Clinical trial of Endovascular treatment of acute ischemic stroke in the Netherlands, a Dutch trial studying the beneficial effects of endovascular treatment of endovascular treatment in patients suffering from acute

ischemic stroke.

NCCT: Non-contrast Computed Tomography.

NHISS: National Institutes of Health Stroke Scale; Measure to describe the degree impairment caused by a stroke.

OR: Odds Ratio; ratio of the odds of an event occurring in one group to the odds of it occurring in another group.

ROI: Region of Interest

SD: Standard Deviation

TAI: Thrombus attenuation increase. Measure of thrombus perviousness as assessed on the combination of non-contrast CT and CTA. This measure assesses the thrombus permeability with a quantitative measure.